NONLINEAR ACOUSTIC RESPONSE OF AN AIRCRAFT FUSELAGE SIDEWALL STRUCTURE BY A REDUCED-ORDER ANALYSIS

Adam Przekop
National Institute of Aerospace
Hampton, Virginia 23666, USA. Email: adam@nianet.org

Stephen A. Rizzi
NASA Langley Research Center, Structural Acoustics Branch
Hampton, Virginia 23681, USA. Email: stephen.a.rizzi@nasa.gov

David S. Groen
The Boeing Company, Phantom Works Structures Technology
St. Louis, Missouri 63166, USA. Email: david.s.groen@boeing.com

ABSTRACT

A reduced-order nonlinear analysis of a structurally complex aircraft fuselage sidewall panel is undertaken to explore issues associated with application of such analyses to practical structures. Of primary interest is the trade-off between computational efficiency and accuracy. An approach to modal basis selection is offered based upon the modal participation in the linear regime. The nonlinear static response to a uniform pressure loading and nonlinear random response to a uniformly distributed acoustic loading are computed. Comparisons of the static response with a nonlinear static solution in physical degrees-of-freedom demonstrate the efficacy of the approach taken for modal basis selection. Changes in the modal participation as a function of static and random loading levels suggest a means for improvement in the basis selection.

INTRODUCTION

Dynamic response analysis tools used by the aerospace industry rely heavily on a linear approach. Commercial finite element codes make a linear modal frequency response of a complicated structure straightforward, even for large degree-of-freedom (DoF) systems. However, this approach is not suitable for predicting the response of aircraft structures when they respond to high dynamic loading in a geometrically nonlinear manner. A nonlinear dynamic analysis in physical DoFs is computationally prohibitive, especially for non-deterministic problems involving long simulation times. It is common practice to reduce the system size by modeling just a portion of the structure, e.g. a single bay in a multi-bay panel. However, with such an approach, important global dynamics are lost because the boundary conditions can not be accurately modeled in a nonlinear dynamic analysis.

In recognition of the above limitations, there has been significant effort in recent years in the development of finite element based reduced-order nonlinear analysis methods [1-5]. These methods have been numerically and experimentally validated for simple structures including flat and curved beams and plates [6-8]. With the exception of a simple stiffened panel studied

in [3], the application of these reduced-order nonlinear analyses to a practical aerospace structure has been almost non-existent. The purpose of this work is to explore the challenges of applying such methods to typical aircraft structure, i.e. riveted skin-frame-longeron metallic structures with system sizes ranging in the tens of thousands of DoFs. To take advantage of the finite element libraries and pre- and post-processing capabilities of commercial finite element codes, an indirect nonlinear stiffness evaluation procedure is used [9]. The procedure is implemented in the program RANSTEP, for "Reduced order Analysis using a Nonlinear STiffness Evaluation Procedure," for use with MSC.NASTRAN and ABAQUS finite element programs.

In the limit of including all linear eigenvectors in the modal basis, results found using the reduced-order analysis should be identical to those obtained via an analysis in physical DoFs because there is no modal truncation. However, the cost associated with this would likely exceed the cost of the physical DoF analysis we wish to avoid. Since previous results for simpler structures indicated that accurate reduced-order response predictions could be made using an abbreviated modal basis, the focus of the present work is on finding a means of methodically down-selecting the basis from the multitude of candidates. For this purpose, the modal participation factor is considered. All modes need to initially be included in the analysis to determine their modal participation, so that the most significant modes can be retained in the subsequent analyses. In other words, we need to solve the problem the hard way first to determine a more efficient solution for later use. Because of the high cost of computing all nonlinear modal stiffness terms, the modal participation will be assessed using a linear analysis for which the linear stiffness is readily available. Reduced-order nonlinear static and random displacement responses are presented for an aluminum fuselage sidewall panel. The static solution is compared with an analysis in physical DoFs to determine the effect of modal truncation as the response increases from essentially linear to highly nonlinear. The static comparison helps deduce the effect of modal truncation on the random response where a physical DoF analysis is not available.

REDUCED-ORDER NONLINEAR FINITE ELEMENT ANALYSIS

The equations of motion of the nonlinear system in physical DoF can be written as

$$\boldsymbol{M}\ddot{\boldsymbol{X}}(t)+\boldsymbol{C}\dot{\boldsymbol{X}}(t)+\boldsymbol{F}_{\boldsymbol{NL}}(\boldsymbol{X}(t))=\boldsymbol{F}(t) \tag{1}$$

where $\boldsymbol{M}$ and $\boldsymbol{C}$ are the system mass and damping matrices, $\boldsymbol{F}_{\boldsymbol{NL}}$ is nonlinear restoring force, $\boldsymbol{X}$ is the displacement response vector and $\boldsymbol{F}$ is the force excitation vector, respectively. A set of coupled modal equations with reduced DoFs can be obtained by applying the modal coordinate transformation $\boldsymbol{X}=\boldsymbol{\Phi q}$ to Equation (1), where $\boldsymbol{q}$ is the modal displacement response vector. The modal basis matrix $\boldsymbol{\Phi}$ is formed from the selected eigenvectors obtained from a linear eigenanalysis. Generally, a small set of L basis functions are included giving

$$\tilde{\boldsymbol{M}}\ddot{\boldsymbol{q}}(t)+\tilde{\boldsymbol{C}}\dot{\boldsymbol{q}}(t)+\tilde{\boldsymbol{F}}_{\boldsymbol{NL}}(q_1(t),q_2(t),\ldots,q_L(t))=\tilde{\boldsymbol{F}}(t) \tag{2}$$

where, for mass-normalized eigenvectors,

$$\tilde{\boldsymbol{M}}=\boldsymbol{\Phi}^T\boldsymbol{M}\boldsymbol{\Phi}=\lceil\boldsymbol{I}\rfloor \qquad \tilde{\boldsymbol{C}}=\boldsymbol{\Phi}^T\boldsymbol{C}\boldsymbol{\Phi}=\lceil 2\zeta_r\omega_r\rfloor \qquad \tilde{\boldsymbol{F}}_{NL}=\boldsymbol{\Phi}^T\boldsymbol{F}_{NL} \qquad \tilde{\boldsymbol{F}}=\boldsymbol{\Phi}^T\boldsymbol{F} \tag{3}$$

and ω_r are the undamped natural frequencies and ζ_r are the viscous damping factors. The nonlinear modal restoring force $\tilde{\boldsymbol{F}}_{\boldsymbol{NL}}$ can be expressed in terms of linear, d, quadratic nonlinear, a, and cubic nonlinear, b, modal stiffness coefficients as [9]

$$\tilde{F}_{NL}(q_1, q_2, \ldots, q_L) = \sum_{j=1}^{L} d_j^r q_j + \sum_{j=1}^{L}\sum_{k=j}^{L} a_{jk}^r q_j q_k + \sum_{j=1}^{L}\sum_{k=j}^{L}\sum_{l=k}^{L} b_{jkl}^r q_j q_k q_l \qquad r = 1, 2, \ldots, L \tag{4}$$

This form of $\tilde{\boldsymbol{F}}_{\boldsymbol{NL}}$ reduces the problem of determining the linear and nonlinear stiffness coefficients to a series of nonlinear static problems with a series of different prescribed displacement fields formed as a combination of eigenvectors. The number of required displacement fields and nonlinear static solutions required to determine the nonlinear stiffness coefficients is given by [9]

$$\text{Number of Static Solutions} = 3\binom{L}{1} + 3\binom{L}{2} + \binom{L}{3} \tag{5}$$

where

$$\binom{L}{n} = \frac{L!}{n!(L-n)!} \tag{6}$$

Since the number of nonlinear static solutions increases rapidly as the number of basis functions L increases, there exists a trade-off between the solution accuracy and computational effort. These considerations will be discussed later in the paper.

Once the nonlinear stiffness terms are fully determined, Equation (2) is numerically integrated using a 4th order Runge-Kutta scheme [9] to determine the modal displacement time history. Physical displacements are reconstructed using the inverse modal coordinate transform.

FUSELAGE SIDEWALL PANEL

A section of a previously studied fuselage sidewall panel [10] served as the basis for the panel considered in the present study. The MSC.NASTRAN FE model of the panel section is presented in Figure 1. The skin panel measures 58.11 in. by 25.06 in. and is subdivided by a riveted frame and longeron substructure into nine bays in 3-by-3 configuration. Each of the nine bays measures 16.75 in. by 7.5 in. between rivet lines. The skin panel, frame and longeron substructures are modeled using 14,832 CQUAD4 plate elements. The thickness of the skin panel and frame L and Z-sections is 0.05 in., while the thickness of the longerons is 0.04 in. A total of 784 rivets attach the frame and longeron substructures to the skin panel, attach the frame L and Z-sections to each other, and attach the longerons to the frames at the intersection points, as indicated in Figure 1. Each rivet is modeled using a single CBEAM beam element. The edges of the skin panel are simply supported with three fixed displacement DoFs and three free rotational DoFs. The entire model contains a total of 96,156 DoFs, 95,352 of which are unconstrained. The following material properties for aluminum were used:

$$E = 10.5 \times 10^6\ psi, \qquad \mu = 0.33, \qquad \rho = 2.614 \times 10^{-4}\ \frac{lb_f - s^2}{in^4}$$

Special modeling considerations. It is a common practice in FE model development to model rivets as rigid kinematic couplings between the nodes being connected. The indirect stiffness evaluation procedure as currently implemented in RANSTEP, however, precludes such modeling, since it involves enforcing arbitrary displacement fields on the FE model [4]. Since it is not a valid operation to prescribe displacements at the both ends of a rigid element [11], the rivets were modeled with beam elements as indicated above. A static analysis of sidewall panels with rivets modeled as both kinematic couplings and CBEAM elements gave

essentially the same displacement response. Therefore, the use of CBEAM elements in lieu of kinematic couplings for rivets did not significantly affect the results.

Modes classification. It is sometimes helpful to classify modes by their spatial characteristics to facilitate the discussion. Several classifications of basis functions used in this reduced order analysis approach have been previously offered for simple symmetric structures [7, 8]. For a complicated structure which does not preserve symmetry, these classifications are not relevant. However, examination of the eigenvectors obtained for the fuselage sidewall panel led to an observation that the modes can be classified into three other categories; global, local and substructure modes. Global modes are generally low frequency modes whose shapes are not significantly influenced by the substructure. Figure 2 shows the lowest global mode of the panel. Local modes are ones in which the substructure is stiff relative to the individual bays. Hence, each bay responds independent of the global motion, as shown in Figure 3. Substructure modes are those modes dominated by the motion of the substructure, as shown in Figure 4. A great number of modes defy this simplistic classification, and may exhibit mixed characteristics of two or more of the basic classification. For example, the mode shown in Figure 5 exhibits characteristics of both a local and a substructure mode.

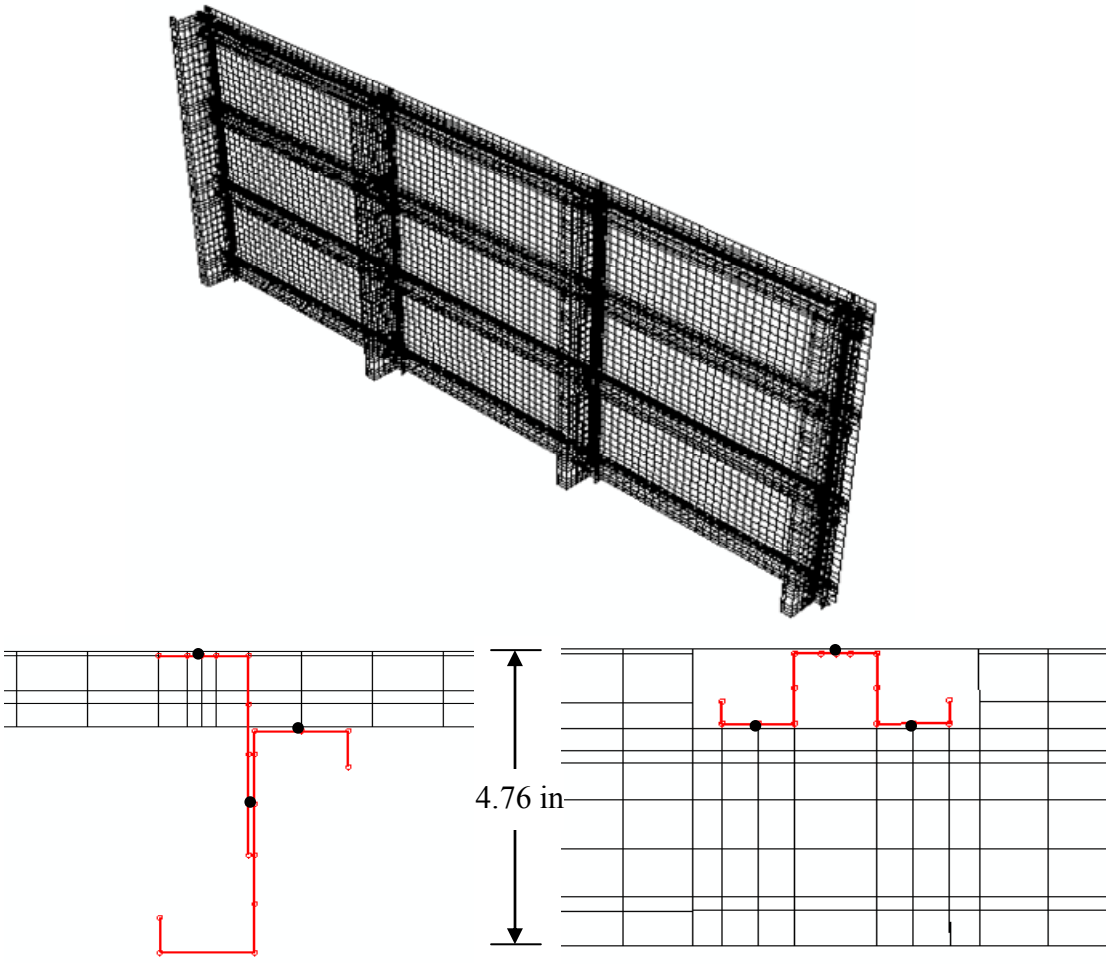

Figure 1: Finite element model of multi-bay fuselage sidewall panel. Rivet locations are indicated with the symbol •.

STATIC RESPONSE

As previously indicated, a nonlinear dynamic analysis of the panel in physical DoFs was prohibitive because of the model size. Therefore, a nonlinear static analysis was first performed so that results from the reduced order nonlinear analysis could be compared with those obtained from a nonlinear static analysis in physical DoFs. The static response analysis is useful because it helps to isolate differences between the physical and reduced-order stiffness.

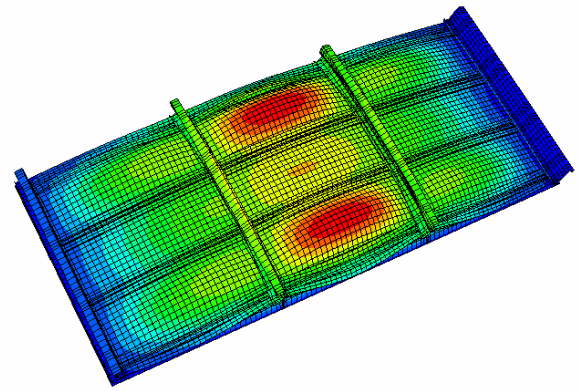

Figure 2: Global mode (Mode 1 – 68.13 Hz)

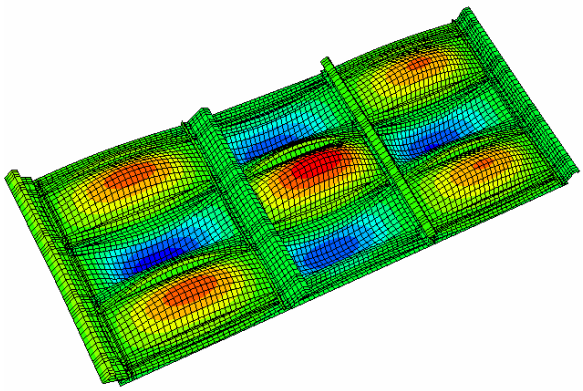

Figure 3: Local mode (Mode 6 – 122.3 Hz)

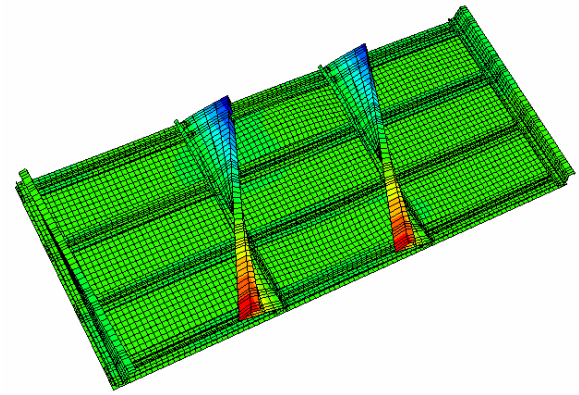

Figure 4: Substructure mode (Mode 7 – 124.9 Hz)

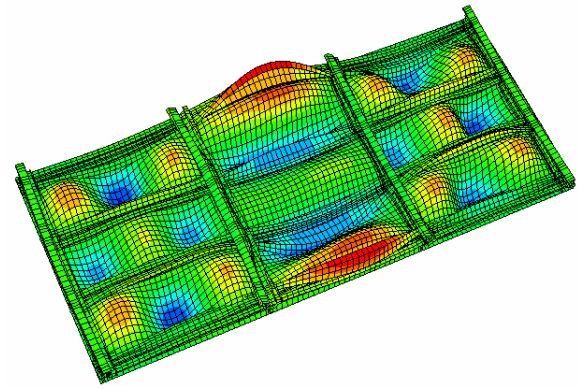

Figure 5: Mixed local-substructure mode (Mode 37 – 271.4 Hz).

Quasi-static loading. A uniformly distributed pressure load was applied to the outside skin surface. Five loading levels were considered, resulting in a nearly linear response at 0.01 psi to highly nonlinear response at 1.00 psi. The load was applied in a quasi-static fashion by ramping it up from zero magnitude at time zero to the specified maximum level at 1.6384s. An additional 0.5s of constant loading was applied at the maximum level to allow any transient behavior to decay, giving the quasi-static modal response at 2.1384s. This loading scheme allowed the same solution procedure to be used for both static and random analyses.

Modal participation factor. For a simple structure, basis function selection is often quite intuitive, given available closed-form solutions, symmetry of the structure and/or loading, boundary conditions, low modal density, etc. For the non-symmetric multi-bay panel considered, the choice is less obvious. Therefore, a more methodical approach using the

modal participation factor, v_r, was utilized. The modal participation factor provides a compact measure of the participation of the r^{th} mode in an expansion utilizing L modes and is expressed as

$$v_r^L = \frac{|q_r|}{\sum_{n=1}^{L} |q_n|} \times 100\% \tag{7}$$

The cumulative modal participation is the sum of the largest S modal participation factors, i.e.,

$$\chi_S^L = \sum_{n=1}^{S} v_n^L \tag{8}$$

By computing v_r for each of L modes, the S modes with the highest participation are easily identified. Those at or above a particular level can be included in subsequent analyses. The benefit of using this approach is that the modal basis selection is not affected by a physical location or DoF of interest. It avoids the situation in which a poor choice of physical location or DoF, e.g. on a nodal line, adversely influences the basis selection. On the other hand, since the modal displacement response must be computed, v_r and χ_S are load-specific, so a basis selection made at one level and distribution of applied loading may not perform well at a different level or distribution. As will be shown, such is the case when the basis selection is made in the linear response regime and applied in the nonlinear regime.

Modal basis selection. The NASTRAN eigenanalysis (solution 103) indicated 89 modes in the frequency range 0–500 Hz. This bandwidth was selected for consistency with the random analysis that follows. A nonlinear modal reduction utilizing all 89 modes was not feasible, since it would involve obtaining 125,759 nonlinear restoring force fields, as per Equation (5). Therefore, a further modal reduction was sought. The following approach was undertaken. A linear modal reduction was first performed utilizing all 89 modes. This operation is computationally expedient as the linear stiffness is obtained directly from the linear eigenanalysis. A uniform pressure of 0.01 psi was then applied in a quasi-static fashion and modal participation factors v_r^{89} were computed for each mode. The modal participation factor for the eight most significant modes was found to be roughly 1.0% or greater, giving a cumulative participation of $\chi_8^{89} = 94.21\%$. The modal participation for the nineteen most significant modes was found to be roughly 0.25% or greater, giving a cumulative participation of $\chi_{19}^{89} = 98.35\%$. A plot of the cumulative participation χ_S^{89} for the highest participating nineteen modes is shown in Figure 6. It is seen that there is a point beyond which the addition of modes yields little added accuracy. At the same time, the number of nonlinear static solutions grows rapidly with each additional mode. The difference between the nineteen and eight-mode cumulative participation is a factor of 1.04, while the number of static nonlinear problems required increases by a factor of 9.38 (from 164 to 1539). Lastly, note the importance of selecting the highest contributing modes. For example, a selection of the lowest nineteen modes versus the nineteen modes with the highest participation yields a cumulative participation of 91.87% compared to 98.35%.

Static displacement response. The static transverse response at the center of the center bay is shown as a function of static pressure load in Figure 7. Three solutions are shown; a linear modal solution including all 89 modes below 500 Hz, a reduced order nonlinear solution (RANSTEP) utilizing nineteen modes, and a NASTRAN nonlinear static solution (solution

106) in physical DoFs. The linear modal solution is applicable at the lowest level of 0.01 psi. As the loading increases, the linear solution becomes excessively conservative compared to the nonlinear analysis in physical DoF. The results obtained via the RANSTEP analysis are shown capable of capturing the nonlinear stiffening effect, although this effect is over-pronounced and results in a non-conservative prediction relative to the physical DoF solution.

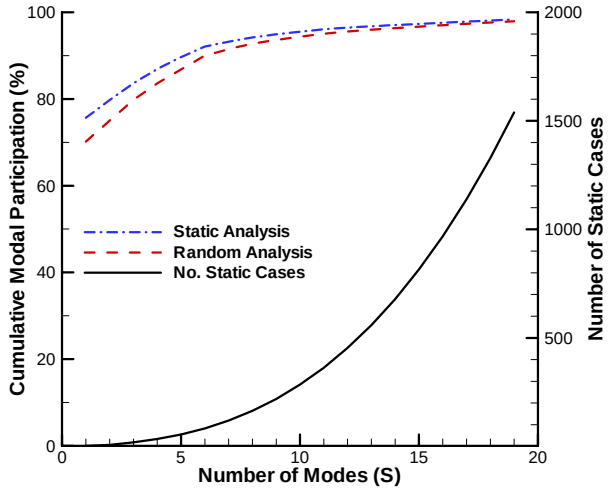

Figure 6: Cumulative participation χ_S^{89} and number of static cases as function of S modes.

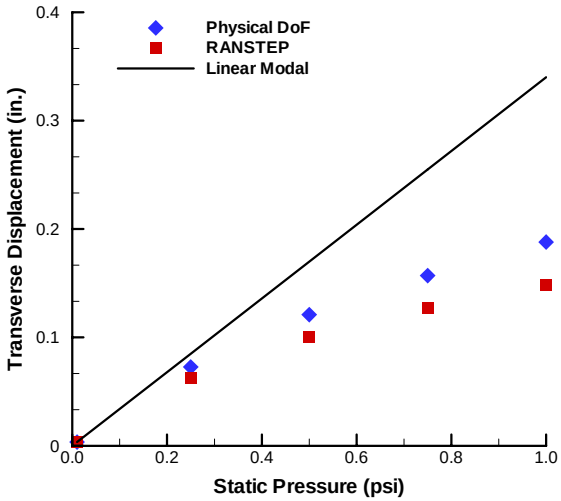

Figure 7: Static transverse displacement response at center of center bay.

To understand the cause of this difference, it is helpful to see how the modal participation changes with increasing load. The nineteen selected mode numbers, frequencies and types (G-global, L-local, S-substructure, LS-mixed local/substructure) are listed in Table 1. The modal participation v_r^{19} is used since computing v_r^{89} would have necessitated 125,759 nonlinear static solutions for the nonlinear regime. At the 1.0 psi loading, it is seen that the participation of the first mode drops dramatically relative to the 0.01 psi loading. Further, the contribution of the higher frequency modes generally increases with increasing load. Therefore, it can be assumed that the modes *not included* in the original selection based on a linear analysis also become increasingly important as the response becomes nonlinear. Since the modal truncation error increases with increasing nonlinearity, it suggests that the basis selection should be performed in the nonlinear regime for increased accuracy. Nevertheless, the results shown demonstrate that the reduced order nonlinear modal simulation captures the salient features of the nonlinear static response for a high-DoF stiffened structure.

RANDOM RESPONSE

Random acoustic loading. A uniformly distributed random pressure load was applied to the outside skin surface. The loading spectrum is shown in Figure 8 and is based on measurements made on a military aircraft at sea level. Loading time histories were generated by summing sine waves with prescribed amplitudes and random phase, within the specified bandwidth using a discrete inverse Fourier transform. A sharp roll-off of the input spectrum at the cut-off frequency of f_c = 500 Hz practically eliminates direct excitation of the structure outside the frequency range of interest. Seven loading levels were considered to span the response regime from essentially linear (106 dB OASPL or 5.567×10^{-3} psi RMS) to highly nonlinear (160 dB OASPL or 0.29 psi RMS). At each level, ten separate loading time histories, each with a 2.1384s duration, were generated for ensemble averaging.

Table 1: Modal participation factors v_r^{19} obtained from the static analysis.

Mode No.	Mode Type	Frequency (Hz)	Pressure Loading (psi)	
			0.01	1.0
1	G	68.1	76.94	56.46 ↓
2	G	99.5	0.26	0.18 ↓
5	S	118.8	2.81	3.21 ↑
6	L	122.3	0.73	0.51 ↓
7	S	124.9	3.94	5.18 ↑
9	LS	126.1	0.62	1.06 ↑
10	LS	128.9	0.31	0.73 ↑
13	L	135.8	0.25	6.84 ↑
15	LS	147.7	3.33	4.21 ↑
16	LS	157.4	4.17	5.30 ↑
20	L	195.3	0.28	0.93 ↑
21	L	196.1	0.25	1.30 ↑
25	L	211.2	2.47	2.89 ↑
26	L	220.6	0.56	0.55 ↓
28	L	238	0.98	0.19 ↓
37	LS	271.4	0.26	1.63 ↑
40	L	279.9	0.40	2.35 ↑
41	L	280.5	0.27	2.87 ↑
46	L	304.5	1.15	3.61 ↑

Modal participation and basis selection. A linear reduced order modal simulation was performed at a very low excitation level of 106 dB OASPL to assess the modal participation. The simulation utilized all 89 modes present in the bandwidth of interest. For the random loading, the modal participation v_r may be written as

$$v_r^L = \frac{RMS\left(q_r\right)}{\sum_{n=1}^{L} RMS\left(q_n\right)} \times 100\% \tag{9}$$

Like the static case, the same eight and nineteen modes were found to exceed 1.0% and 0.25% of v_r^{89}, respectively, but with slightly different modal participation factors. The cumulative modal contribution of the most significant eight modes was found to be $\chi_8^{89} = 92.78\%$, and that of the most significant nineteen modes was found to be $\chi_{19}^{89} = 97.95\%$. In other words, at the 106 dB excitation level, the truncated 81 modes for the eight-mode solution represented 7.22% of cumulative contribution, while the 70 truncated for the nineteen-mode solution

represented 2.05% of cumulative contribution. The cumulative participation χ_S^{89} for the most significant nineteen modes is also shown in Figure 6 and resembles the behavior of the static condition.

Random displacement response. For the random response analysis, a mass proportional damping corresponding to 2.0% critical damping for the fundamental mode was specified. The Runge-Kutta integration used a fixed integration time step between 50μs (for the lowest excitation levels) and 5μs (for the highest excitation levels). The first 0.5s of each response record was discarded to remove the initial transient response, resulting in response histories of 1.6384s in duration. For each simulation, the modal response was stored at every 50μs, giving time records of 32,768 points.

The RMS transverse displacement response at the center of the center bay is shown in Figure 9. The linear modal results were obtained using all 89 modes, and the reduced order nonlinear RANSTEP results were obtained using nineteen modes. The nonlinear behavior is as expected, with the onset of geometrically nonlinear response emerging in the range between 136 dB OASPL (0.0178 psi) and 142 dB OASPL (0.0356 psi).

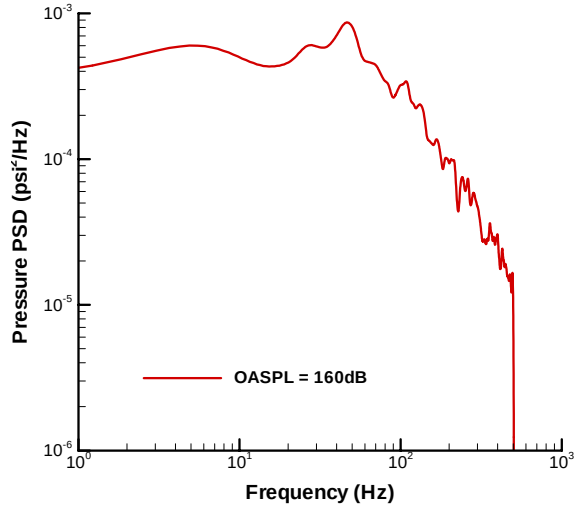

Figure 8: Random pressure loading spectrum.

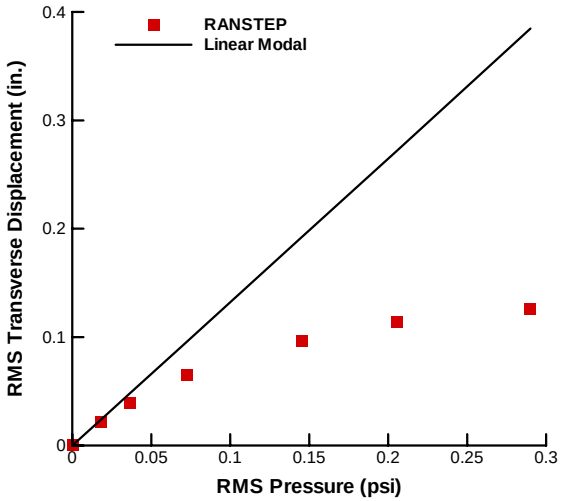

Figure 9: RMS transverse displacement response at center of center bay.

Transverse displacement PSDs at the center of the center bay were obtained from linear and nonlinear modal simulations at low (106 dB), moderate (136 dB), and high (154 dB OASPL or 0.145 psi) levels of acoustic excitations, see Figure 10 to Figure 13. Figure 10 demonstrates that the only difference in the linear response regime is attributable to modal truncation above the highest selected mode at 304.5 Hz. Figure 11 illustrates why an analysis of a single panel is problematic even in the linear response regime. The linear modal response shown was obtained from the full multi-bay panel analysis and is identical to that presented in Figure 10. Overlaid are responses obtained from physical DoF analyses of a single panel having the same dimensions as the center bay of the full panel, but without substructure. Either fully clamped or simply supported boundary conditions were specified at what would have been the rivet lines. Clearly, neither of the simplified analyses is capable of predicting the response across the full frequency range. While a frequency dependent boundary condition could be developed for the linear regime, no such remedy exists for the nonlinear regime.

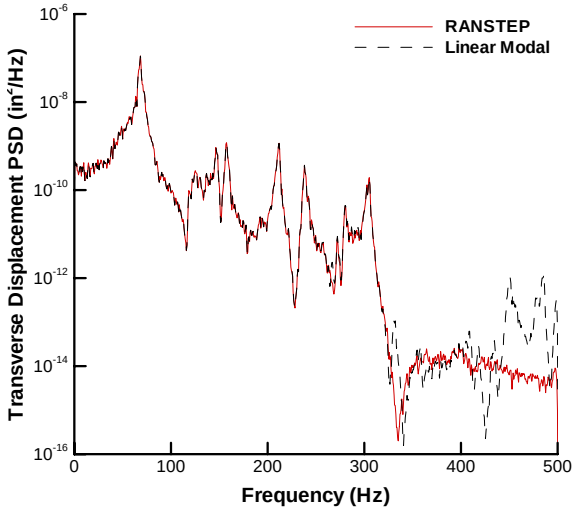

Figure 10: Linear and nonlinear transverse displacement PSD at 106 dB OASPL.

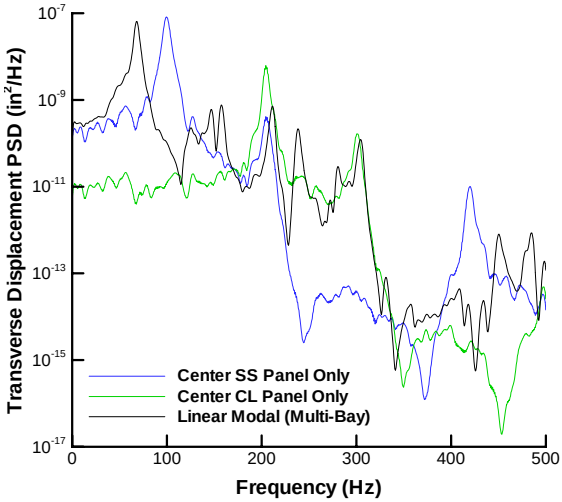

Figure 11: Comparison of multi-bay panel and center bay analyses at 106 dB OASPL.

Figure 12 shows that as the excitation level increases to 136 dB, the PSD peaks resulting from the nonlinear analysis begin to shift toward higher frequencies and to broaden relative to the linear analysis. Nonlinear versus linear PSD peaks cross-identification, however, remains possible at this level. This level of nonlinearity is comparable to the highest level studied for a much thicker panel in reference [3]. In the highly nonlinear response regime, Figure 13, peak cross-identification is no longer possible. The response is dominated by one broad washed-out peak, which likely originates from several modes included in the analysis.

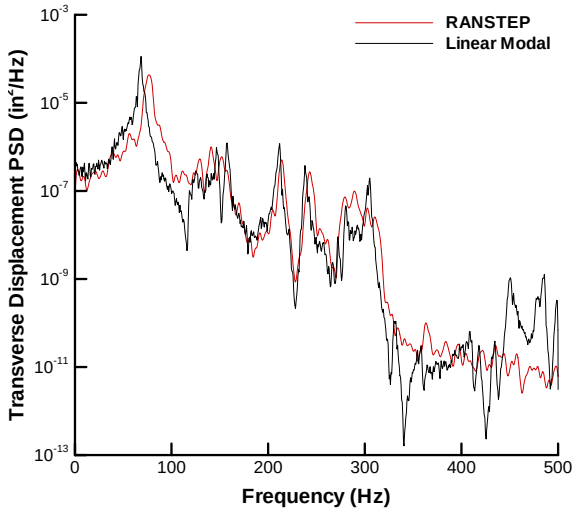

Figure 12: Linear and nonlinear transverse displacement PSD at 136 dB OASPL.

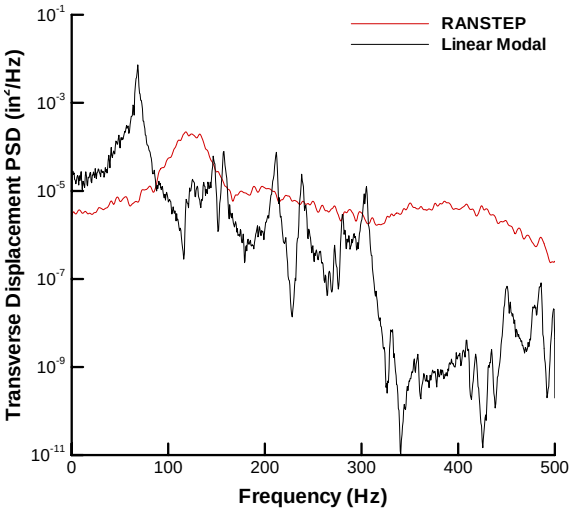

Figure 13: Linear and nonlinear transverse displacement PSD at 154 dB OASPL.

It is helpful to investigate how the modal participation changes as a function of response level. Table 2 provides the modal participations v_r^8 and v_r^{19} at three load levels. As the loading increases, the participation of the fundamental mode decreases in favor of greater participation of higher frequency modes. For example, $v_{13}^{19} = 0.35\%$ at 106 dB, but increases to 6.42% at 154 dB. Furthermore, in the linear response regime (106 dB), v_r^8 and v_r^{19} are very similar for the modes that are included in both analyses, indicating that modal convergence has been

achieved. However, as the loading increases, v_r^8 and v_r^{19} begin to vastly differ due to modal truncation. As in the static case, this suggests that the basis selection should be performed in the nonlinear regime for increased accuracy. Unfortunately, this requires solving the problem once the hard way, i.e., solving for all nonlinear modal stiffness terms and integrating the larger coupled system to obtain the modal participation, so that subsequent analyses can be performed more efficiently with a reduced basis.

Table 2: Modal participation factors v_r^8 and v_r^{19} obtained at different loading levels.

Mode	106 dB		136 dB		154 dB	
	v_r^8	v_r^{19}	v_r^8	v_r^{19}	v_r^8	v_r^{19}
1	75.65	71.64	74.06 ↓	63.16 ↓	56.35 ↓	38.57 ↓
2		0.30		0.92 ↑		3.08 ↑
5	3.44	3.26	3.27 ↓	2.52 ↓	5.72 ↑	4.04 ↑
6		0.87		1.72 ↑		3.49 ↑
7	5.13	4.86	5.32 ↑	4.87 ↔	4.93 ↓	4.04 ↓
9		0.78		1.44 ↑		2.88 ↑
10		0.41		1.34 ↑		3.08 ↑
13		0.35		3.07 ↑		6.42 ↑
15	4.12	3.90	5.24 ↑	4.48 ↑	7.55 ↑	4.85 ↑
16	5.23	4.95	4.09 ↓	3.61 ↓	6.79 ↑	4.21 ↑
20		0.38		0.79 ↑		2.37 ↑
21		0.32		1.14 ↑		2.77 ↑
25	3.45	3.27	3.88 ↑	3.29 ↔	5.55 ↑	2.74 ↓
26		0.67		0.77 ↑		2.34 ↑
28	1.36	1.29	1.88 ↑	1.51 ↑	4.58 ↑	2.69 ↑
37		0.32		1.36 ↑		3.29 ↑
40		0.53		0.96 ↑		2.90 ↑
41		0.36		1.49 ↑		3.27 ↑
46	1.61	1.53	2.26 ↑	1.55 ↔	8.53 ↑	2.97 ↑

CONCLUDING REMARKS

A nonlinear reduced-order static and random response analysis of a typical aircraft fuselage sidewall panel was presented. The reduced-order static analysis captured the essential features of the nonlinear behavior, but over-predicted the effect of nonlinearity compared with a solution in physical DoFs. The reduced-order random response analysis was shown to predict the expected behavior, but quantitative comparisons with a physical DoF solution were not available due to their prohibitive computational cost.

The modal participation was found to change as a function of the nonlinear response. The participation of the lowest, most dominant mode decreased with increasing nonlinearity, while that of the higher frequency modes increased. Therefore, a converged modal basis obtained via a linear analysis produced truncation error in the nonlinear response regime. Consequently, an alternative means of identifying the modal participation in the nonlinear regime is needed without the expense of computing the full set of nonlinear modal stiffness terms. This is an area requiring further study.

REFERENCES

[1] Mei, C., Dhainaut, J.M., Duan, B., Spottswood, S.M., and Wolfe, H.F., "Nonlinear random response of composite panels in an elevated thermal environment," Air Force Research Laboratory, Wright-Patterson Air Force Base, OH, AFRL-VA-WP-TR-2000-3049, October 2000.

[2] Przekop, A., Guo, X., Azzouz, M.S., and Mei, C., "Reinvestigation of nonlinear random response of shallow shells using finite element modal formulation," *Proceedings of the 45th AIAA/ASME/ASCE/AHS/ASC Structures, Structural Dynamics and Materials Conference*, AIAA-2004-1553, Palm Springs, CA, 2004.

[3] McEwan, M.I., Wright, J.R., Cooper, J.E., and Leung, Y.T., "A finite element/modal technique for nonlinear plate and stiffened panel response prediction," *Proceedings of the 42nd AIAA/ASME/ASCE/AHS/ASC Structures, Structural Dynamics, and Materials Conference*, AIAA-2001-1595, Seattle, WA, 2001.

[4] Muravyov, A.A. and Rizzi, S.A., "Determination of nonlinear stiffness with application to random vibration of geometrically nonlinear structures," *Computers and Structures*, Vol. 81, No. 15, pp. 1513-1523, 2003.

[5] Mignolet, M.P., Radu, A.G., and Gao, X., "Validation of reduced order modeling for the prediction of the response and fatigue life of panels subjected to thermo-acoustic effects," *Structural Dynamics: Recent Advances, Proceedings of the 8th International Conference*, Southampton, UK, 2003.

[6] Hollkamp, J.J., Gordon, R.W., and Spottswood, S.M., "Nonlinear sonic fatigue response prediction from finite element modal models: a comparison with experiments," *Proceedings of the 44th AIAA/ASME/ASCE/AHS/ASC Structures, Structural Dynamics, and Materials Conference*, AIAA-2003-1709, Norfolk, VA, 2003.

[7] Rizzi, S.A. and Przekop, A., "The effect of basis selection on static and random response prediction using nonlinear modal simulation," NASA TP-2005-213943, December 2005.

[8] Przekop, A. and Rizzi, S.A., "Nonlinear reduced order random response analysis of structures with shallow curvature," *To appear in the AIAA Journal*, 2006.

[9] Rizzi, S.A. and Przekop, A., "Estimation of sonic fatigue by a reduced order finite-element-based analysis," *Structural Dynamics: Recent Advances, Proceedings of the 9th International Conference*, Southampton, UK, 2006.

[10] Buehrle, R.D., Fleming, G.A., Pappa, R.S., and Grosveld, F.W., "Finite element model development for aircraft fuselage structures," *Sound and Vibration Magazine*, Vol. 35, No. 1, pp. 32-38, 2001.

[11] "MSC.NASTRAN 2005 Quick Reference Guide," MSC.Software Corporation, 2004.